LA-UR-87-2198

Los Alamos National Laboratory is operated by the University of California for the United States Department of Energy under contract W-7405-ENG-36

LA-UR--87-2198

DE87 011733

TITLE: HIGH-STRAIN-RATE DEFORMATION MECHANISMS IN COPPER AND IMPLICATIONS FOR BEHAVIOR DURING SHOCK-WAVE DEFORMATION

AUTHOR(S): P. S. Follansbee, MST-5

SUBMITTED TO 1987 APS Topic Conference on Shockwaves in Condensed Matter, Monterey, California, July 20-23, 1987

DISCLAIMER

Los Alamos National Laboratory
Los Alamos, New Mexico 87545

GH-STRAIN-RATE DEFORMATION MECHANISMS IN COPPER AND IMPLICATIONS FOR BEHAVIOR RING SHOCK-WAVE DEFORMATION

ul S. FOLLANSBEE

s Alamos National Laboratory, Los Alamos, NM, 87545, USA

recently developed model for the deformation of copper is reviewed. The model separates e kinetics of structure evolution from those at constant structure and uses the mechanical reshold stress (yield stress at 0 K) as an internal-state variable. Predictions of the ress-strain behavior at high strain rates are compared with experimental results, and the tential application of the modeling procedure in the shock-wave regime is discussed.

Final Text & Figures

Not final copy

1. INTRODUCTION

The study of the shock deformation of metals has been a topic of long-standing interest. Much of the previous interest has centered on establishing the pressure/volume relationship in shocked material and there have been several comprehensive reviews in this area[1]. There also has been extensive research into the metallurgical aspects of shock-wave deformation and of microstructural effects in shock-deformed material[2]. It is well known, for instance, that the imposed strain in a shock wave is accommodated through rapid dislocation generation and that deformation twinning and phase transformations may occur[3]. There has been comparatively little work, however, in applying the mechanistic understanding of deformation processes, developed through extensive studies at low strain rates, to models for shock deformation.

The approach of our work has been to study the deformation behavior of metals at strain rates from 10^{-4} s^{-1} to 10^{4} s^{-1} and to develop models or descriptions of this behavior that represent the kinetics of the deformation mechanisms encountered. We concentrate on these "lower" strain rates because the experimental measurement of stress/strain behavior is straightforward at strain rates less than 10^{4} s^{-1}. Our goal is to combine these measurements with a few carefully selected but difficult measurements in the shock-wave regime and to investigate whether the understanding, and in particular the models, developed at the lower strain rates extrapolate into the shock-wave regime. To do this, we must first verify that deformation mechanisms do not change in the higher strain rate regime, or, if they do, we must know how to

introduce these effects into the deformation models.

This paper will review the status of this research. The first section describes one model developed to describe the deformation of copper over a wide range of strain rates. The application of this model to experimental results in copper and stainless steel is presented in the section 2, and, a few comparisons at strain rates beyond those to which the model has been fit, including some results in the shock-wave regime, are given. Finally, in section 3, the model and experimental results are discussed in light of the objectives described above.

2. A MODEL FOR DISLOCATION GLIDE CONTROLLED DEFORMATION

Following Kocks[4] and Mecking and Kocks[5] we model the interaction of the average dislocation with the average obstacle and consider the flow stress at T=0K (in the absence of thermal fluctuations that assist the dislocation past the obstacle) as an internal state variable or structure parameter and call it the mechanical threshold stress σ^* [6]. Depending on the crystal structure and how the material is hardened, the mechanical threshold stress can be separated into several contributions,

$$\sigma^* = \sigma_a^* + \Sigma \sigma_{ti}^* \qquad (1)$$

where σ_a^* is an athermal contribution through long-range interactions, e.g., with grain boundaries, and σ_{ti}^* is a thermal contribution due to short-range interactions with other dislocations, interstitial atoms, dispersoids, etc. For

the case of pure copper, the thermal component is made up only by the interactions of dislocations with other dislocations, and

$$\sigma^* = \sigma_a^* + \alpha\mu b \sqrt{\rho} \qquad (2)$$

where α is a constant of order unity, μ is the temperature and pressure dependent shear modulus, b is the Burgers vector and ρ is the total dislocation density[5,7].

Evolution of the structure parameter σ^* is considered as the balance between dislocation accumulation and dynamic recovery and the strain hardening rate $\theta = d\sigma^*/d\epsilon$ is used to characterize the differential variation of the structure parameter with strain. We assume that the structure will eventually saturate at a strain-rate and temperature dependent stress σ_s^* leading to a zero rate of strain hardening and we model the strain-hardening behavior using an equation of the form

$$\theta = \theta_o \left[1 - F \left(\frac{\sigma^* - \sigma^*}{\sigma_s^* - \sigma_a^*} \right) \right] \qquad (3)$$

where θ_o is the strain-hardening due to dislocation accumulation and the factor F is chosen from experimental results. When F=1, Eq. 3 represents the Voce law[4] and this is a close approximation for the behavior of many materials. The strain-rate and temperature dependence of the saturation stress σ_s^* is introduced using a phenomenological cross-slip model[4,8].

One significant difference between the form of Eq. 3 found to describe the copper results[9] and the stainless steel results over a wide range of strain rates and that used earlier over a limited range of strain rates[4,5] is that at

high strain rates the data fits indicate a strain-rate dependence to the θ_o term, given by

$$\theta = C_1 + C_2 \ln \dot{\epsilon} + C_3 \dot{\epsilon} \quad . \tag{4}$$

The linear term in this expression begins to contribute significantly at strain rates exceeding 3×10^3 s^{-1} which yields the strong increased hardening that has been observed in these materials at high strain rates. The form given by Eq. 4 is a fit to experimental results at strain rates up to 10^4 s^{-1}. The physical basis for this increased hardening rate remains open, but we recently speculated that high stresses developed near yield of an annealed material (when the dislocation density is low and dislocation or phonon drag limits dislocation mobility) could lead to the observed increased hardening rates[10]. Clearly, Eq. 4 can not be valid at strain rates greater than 10^6 s^{-1} because the θ_o term rises above the shear modulus at this strain rate. Thus, the shear modulus becomes the natural limit to the strain-hardening rate due to dislocation accumulation.

To solve for the applied stress σ at any value of the structure parameter, we describe the kinetics of dislocation/obstacle interactions at constant structure with an equation of the form[6]

$$\sigma - \sigma_a^* = s(T, \dot{\epsilon}, P)\, \sigma^* \tag{5}$$

where the strain-rate, temperature, and pressure dependent (through the shear modulus) s gives the ratio between the mechanical threshold stress and applied stress to overcome a specific obstacle. For thermally activated controlled deformation, for instance,

$$\ln \frac{\dot{\epsilon}_o}{\dot{\epsilon}} = \frac{\Delta G(\sigma,\sigma^*)}{kT} = \frac{g_o \mu b^3}{kT}\left[1 - \left(\frac{\sigma - \sigma_a^*}{\sigma^* - \sigma_a^*}\right)^p\right]^q \quad (6)$$

where k is the Boltzmann constant, $\dot{\epsilon}_o$ is a constant, and ΔG is the total activation energy. At high strain rates, the time of travel between separate obstacles, which is limited by drag forces, may become rate limiting, and it is possible that applied stresses greater than the mechanical threshold stress would be required for continued deformation. For this case, which has been treated by several investigators, the relation between strain rate, stress, temperature, and pressure is more complicated; one form is written as

$$\dot{\epsilon} = \frac{\dot{\epsilon}_o}{\frac{MB\alpha\mu b\nu_o}{\sigma b\sigma^*} + \exp\frac{\Delta G}{kT}} \quad (7)$$

where M is a Taylor factor and B is the drag coefficient which is deduced from etch pit or ultrasonic techniques but allowed to vary such that the dislocation velocity remains below the shear wave velocity[10].

Equation 7 gives the factor s required in Eq. 5 which completes the model for dislocation glide controlled deformation in copper. The various constants required for the model have been derived through a fit to an extensive series of compression data over a wide range of strain rates and strains[9]. The model attempts to describe, from a physical basis, the kinetic processes that define strain rate sensitivity and strain hardening in copper. The model assumes isotropy and that stress-state effects can be modeled using, for instance, a von Mises

yield surface. In the next section, some experimental results that demonstrate the use of the model will be presented.

2. COMPARISON WITH SOME EXPERIMENTAL RESULTS

The first example of the use of the formalism developed in the previous section is the application of Eq. 7 at constant structure. A constant structure is developed by starting with material in a uniform microstructural condition (e.g., fully annealed) and deforming (prestraining) samples along a specified temperature, strain rate and strain history. The temperature and strain-rate dependence of the yield stress, measured in these samples using a reload operation or an instantaneous strain-rate or temperature change, can be analyzed according to Eq. 6 to yield the constant structure kinetic information required by Eq. 5. An example of such a correlation is shown in Fig. 1 for three distinct strain and strain-rate histories in copper. The coordinates in this plot are chosen such that straight lines can be drawn through each set of data. The intercept at T=0K yields the mechanical threshold stress.

If the measurements illustrated in Fig. 1 are applied to several strain, temperature, and strain-rate histories it is possible to evaluate the kinetics of the evolution processes. Examples of this for copper have been described previously[9,10].

One essential feature of the modeling procedure outlined in the previous section is that the kinetics of the evolution or hardening process are separated from the kinetics of the constant structure process. An example of the

utility of such a procedure is shown in Fig. 2, which plots the flow stress at ϵ=0.10 and the mechanical threshold stress as a function of strain rate for annealed Nitronic 40 stainless steel. The sudden increase in the flow stress at strain rates exceeding ~10^3 s^{-1} has been seen in many fcc materials and has been interpreted as a change in deformation mechanism. However, the mechanical threshold stress data show the same increase at these strain rates. Thus, at high strain rates the rate of hardening or evolution is increasing (described by Eq. 5) but the deformation mechanism remains the same. This shows that strain is not a valid state parameter; instead, the mechanical threshold stress provides a better basis for the comparison shown in Fig. 2. An example of the variation of the flow stress in copper at constant threshold stress versus strain rate is shown in Fig. 3. A plot at constant strain shows the same increased flow stress levels at strain rates exceeding 10^3 s^{-1} as does the stainless steel data in Fig. 2. But no such increase is shown in Fig. 3; the slight almost linear strain-rate dependence over the entire range of the measurements shown in Fig. 3 verifies that the constant structure deformation behavior is controlled by the thermally activated interactions between dislocations, which is a fairly rate-insensitive (but still rate dependent) process.

2.1. Predictions at Very High Strain Rates and Comparison with Experimental Results

It is straightforward to extrapolate the model and predict stress-strain behavior at higher strain rates. Experimental results for these conditions, however, are more difficult to obtain. One experimental technique capable of measuring stress-strain behavior at very high

strain rates is the oblique impact used by Clifton and coworkers[11]. Two measurements by Clifton[12] at a shear strain rate of 10^6 s^{-1} are shown in Fig. 4, along with our model prediction. The dramatic yield drop predicted is due to the contribution of dislocation drag controlled deformation at low strains when the dislocation density is low. The high yield stresses predicted would likely be relaxed by rapid dislocation generation (i.e., even more rapid than represented by Eq. 4) or by the contribution of another deformation mechanism, such as deformation twinning. Whereas there appears to be a large difference between the measurements and predictions at large strains, the error is actually slight when the stress-state dependence of plastic flow is accounted for through the appropriate Taylor factors. An interesting feature of the experimental and theoretical predictions at these high strain rates is the apparent approach to perfect-viscoplasticity. In the context of the model described earlier, this is due to rapid strain hardening and early saturation at a rate-dependent flow stress.

Another comparison with experiment is shown in Fig. 5, which shows results of Wilkins and Guinan using the Taylor test[13]. The curve identified with these authors is the stress-strain curve found to give the best agreement between computed and measured shape of the recovered copper projectile. Predictions of our model at strain rates of 10^4 and 10^5 s^{-1} are included in this figure; it is evident that the prediction at the higher strain rate agrees well with the behavior deduced by Wilkins and Guinan.

Comparisons in the shock-wave regime are even more difficult to obtain since stress-strain curves must be deduced from particle velocity

measurements, which are relatively rare. Gray and Follansbee[14,15] have shock deformed and soft recovered copper and have measured the mechanical threshold stress as a function of pulse amplitude and duration. The results are summarized in Fig. 6, which shows the variation of the mechanical threshold stress with strain rate at a strain of 0.0825, equivalent to the transient strain obtained in a 10 GPa shock wave. Results measured in the shock regime are shown in the cross-hatched area. The shock does not yield a uniform strain rate, which gives the uncertainty in strain rate, and in these experiments the threshold stress was found to vary with the pulse duration, which gives the height of the box noted. Predictions for the dependence of the mechanical threshold stress with strain rate are shown by the solid curve. The agreement between the predictions and measurements is not good. However, the predictions are for monotonic deformation, i.e., deformation in one direction and at one strain rate, whereas the shock yields a distinct strain reversal. Gray and Follansbee likened the shock to a one-cycle fatigue test and argued that the strain reversal may lead to reversed plastic flow and a lower rate of dislocation storage than for monotonic loading at the same strain rate[14]. Thus, the solid curve in Fig. 6 may indicate a limiting value for the mechanical threshold stress for monotonic loading. Although consistent with the experimental results, the detailed description of the strain reversal requires a more complicated model than has been proposed here.

3. DISCUSSION

One reason for the lack of success in applying in the shock regime constitutive laws

developed for low strain rate deformation is that the standard constitutive laws, e.g., power-law hardening and strain-rate sensitivity do not adequately represent the kinetics of the deformation processes. The more physically-based constitutive formulation outlined here appears to offer some potential for application to shock-wave deformation. However, there are several differences between shock-wave deformation and deformation at low strain rates that need to be addressed. One difference is that deformation in the shock regime is not volume conserving. This does not influence the procedures outlined above, but it will affect how they are implimented. The high pressures in a shock wave will affect the constitutive behavior through their influence on the shear modulus (primarily through Eq. 2). This is an important observation that should find application to the study of shock-wave deformation.

Finally, in order to employ the formalism presented in this paper, it must be verified that the deformation mechanisms during the high strain rate or shock-wave conditions are those that have been modeled. This requires extensive post-mortem micro-structural characterization[2]. It is known, for instance, that at high shock pressures many materials begin to deform by deformation twinning, which is a much less strain-rate sensitive process than is dislocation glide. One of the goals of our program is to learn how to incorporate such a change in deformation mechanism into the modeling procedure.

REFERENCES

1. R.J. McQueen, S.P. Marsh, J.W. Taylor, J.N. Fritz and W.J. Carter, in: High Velocity Inpact Phenomena, ed. R. Kinslow (Academic Press, New York, 1970) pp.294-417.

2. L.E. Murr, in: Shock Waves and High-Strain-Rate Phenomena in Metals, eds. M.A. Meyers and L.E. Murr (Plenum Press, New York, 1980) pp. 607-673.

3. W.C. Leslie, in: Metallurgical Effects at High Strain Rates, eds. R.W. Rohde, B.M. Butcher, J.R. Holland, C.H. Karnes (Plenum Press, New York, 1973) pp. 571-586.

4. U.F. Kocks, ASME J. Engr. Mat. Tech. 98 (1976) 76.

5. H. Mecking and U.F. Kocks, Acta Metall. 29 (1981) 1865.

6. U.F. Kocks, A.S. Argon and M.F. Ashby, Thermodynamics and Kinetics of Slip, Prog. Mat. Sci. 19 (Pergamon Press, N.Y., 1975).

7. P.S. Follansbee, in: Metallurgical Applications of Shock-Wave and High-Strain-Rate Phenomena, eds. L.E. Murr, K.P. Staudhammer, and M.A. Meyers (Marcel Dekker, Inc., 1986) pp. 451-479.

8. P. Haasen, Phil. Mag. 3 (1958) 384.

9. P.S. Follansbee and U.F. Kocks, Acta Metall. in press.

10. P.S. Follansbee, The rate dependence of structure evolution in copper and its influence on the stress-strain behavior at very high strain rates, in: IMPACT'87, Proc. of the Int. Conf., in press.

11. R.J. Clifton, A. Gilat, and C.-H. Li, in: Material Behavior Under High Stress and Ultrahigh Loading Rates, eds. J. Mescall and V. Weiss (Plenum, N.Y., 1983) pp. 1-19.

12. R.J. Clifton, Unpublished research, Division of Engineering, Brown Univ., Providence, RI.

13. M.L. Wilkins and M.W. Guinan, J. Appl. Phys. 44 (1973) 1200.

14. G.T. Gray III and P.S. Follansbee, Influence of peak pressure and pulse duration on substructure development and threshold stress measurements in shock-loaded copper, in: IMPACT'87, Proc. of Int. Conf., in press.

15. P.S. Follansbee and G.T. Gray III, in: Shock Waves in Condensed Matter, ed. Y.M. Gupta, (Plenum Press, New York, 1986) pp. 371-376.

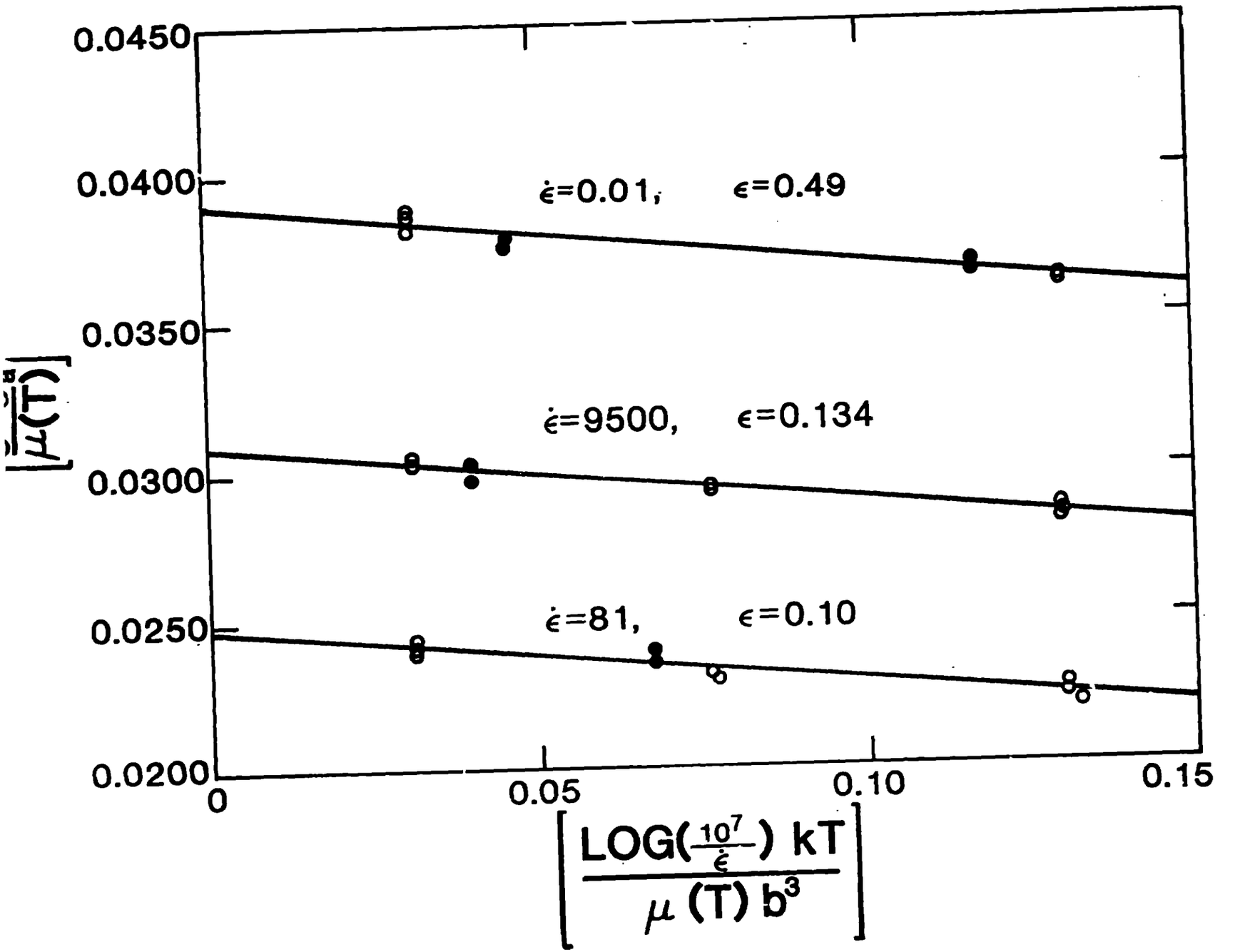
0.0450
0.0400
0.0350
0.0300
0.0250
0.0200
$\dot{\epsilon}$=0.01, ϵ=0.49
$\dot{\epsilon}$=9500, ϵ=0.134
$\dot{\epsilon}$=81, ϵ=0.10
$\left[\frac{\tilde{\mu}(T)}{\mu}\right]$
0
0.05
0.10
0.15
$\left[\frac{\text{LOG}(\frac{10^7}{\dot{\epsilon}})\ kT}{\mu\,(T)\,b^3}\right]$

(7)

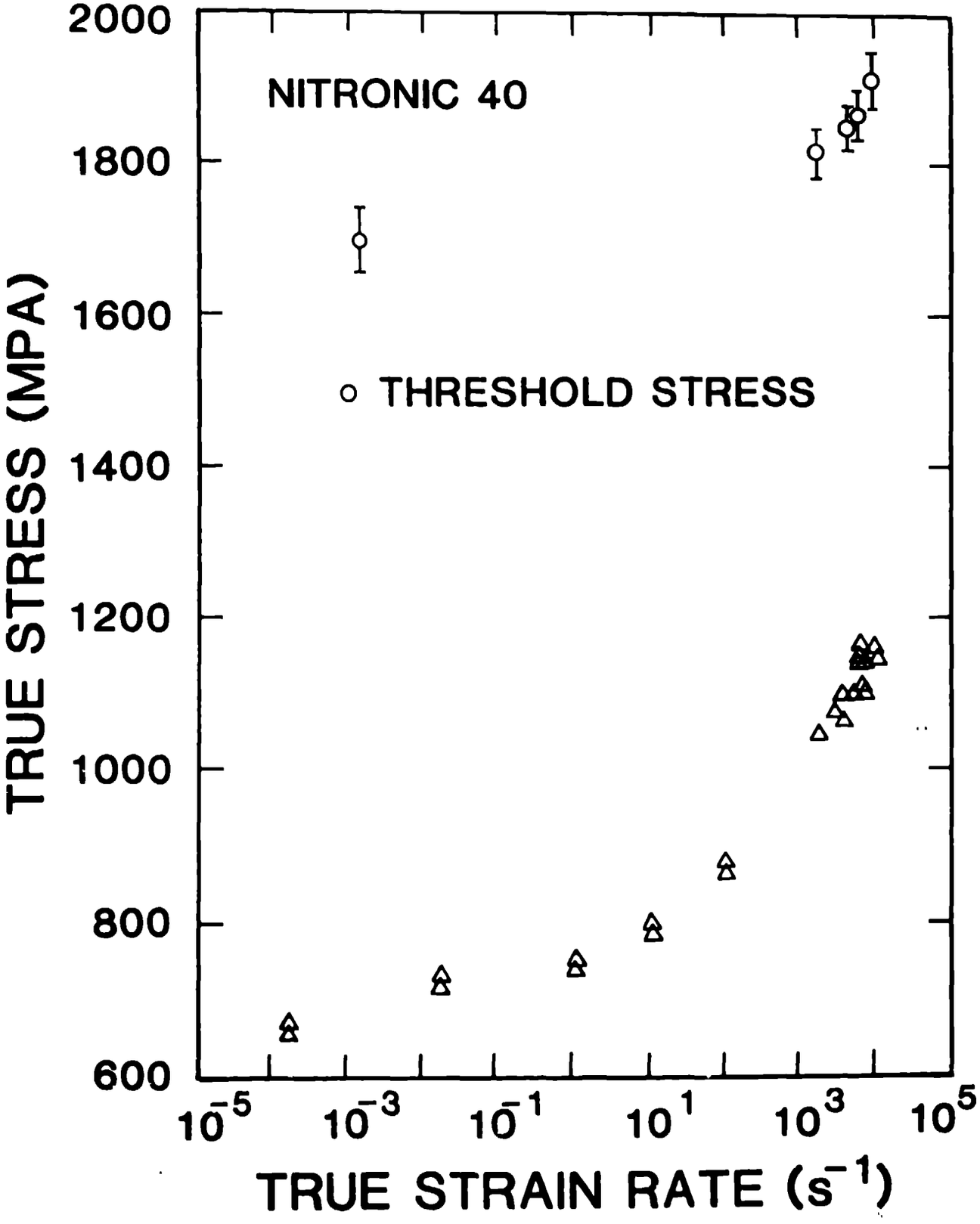
NITRONIC 40
THRESHOLD STRESS
TRUE STRESS (MPA)
2000
1800
1600
1400
1200
1000
800
600
10^{-5}
10^{-3}
10^{-1}
10^{1}
10^{3}
10^{5}
TRUE STRAIN RATE (s^{-1})

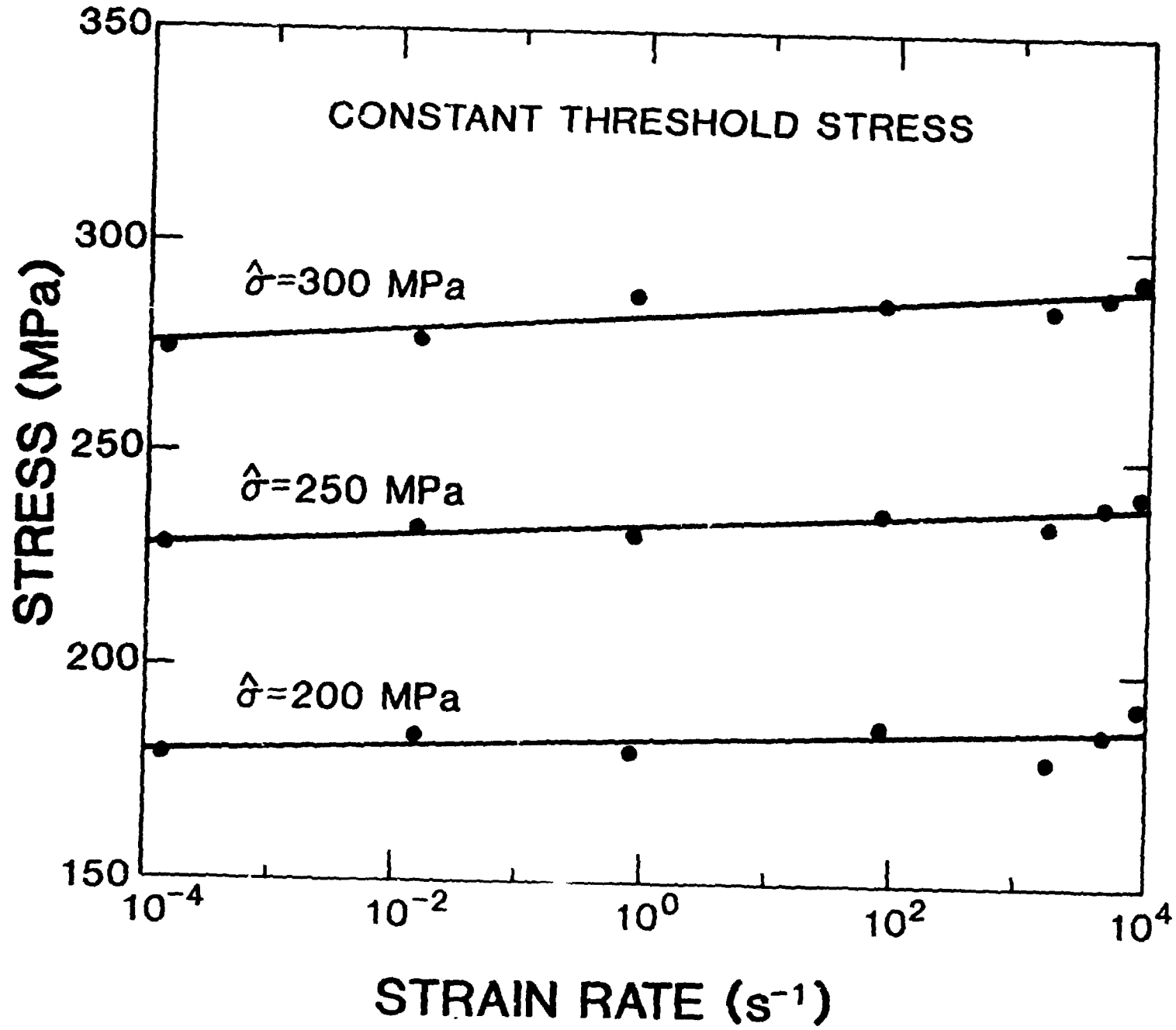
CONSTANT THRESHOLD STRESS
$\hat{\sigma}$=300 MPa
$\hat{\sigma}$=250 MPa
$\hat{\sigma}$=200 MPa
350
300
250
200
150
STRESS (MPa)
10^{-4}
10^{-2}
10^{0}
10^{2}
10^{4}
STRAIN RATE (s^{-1})

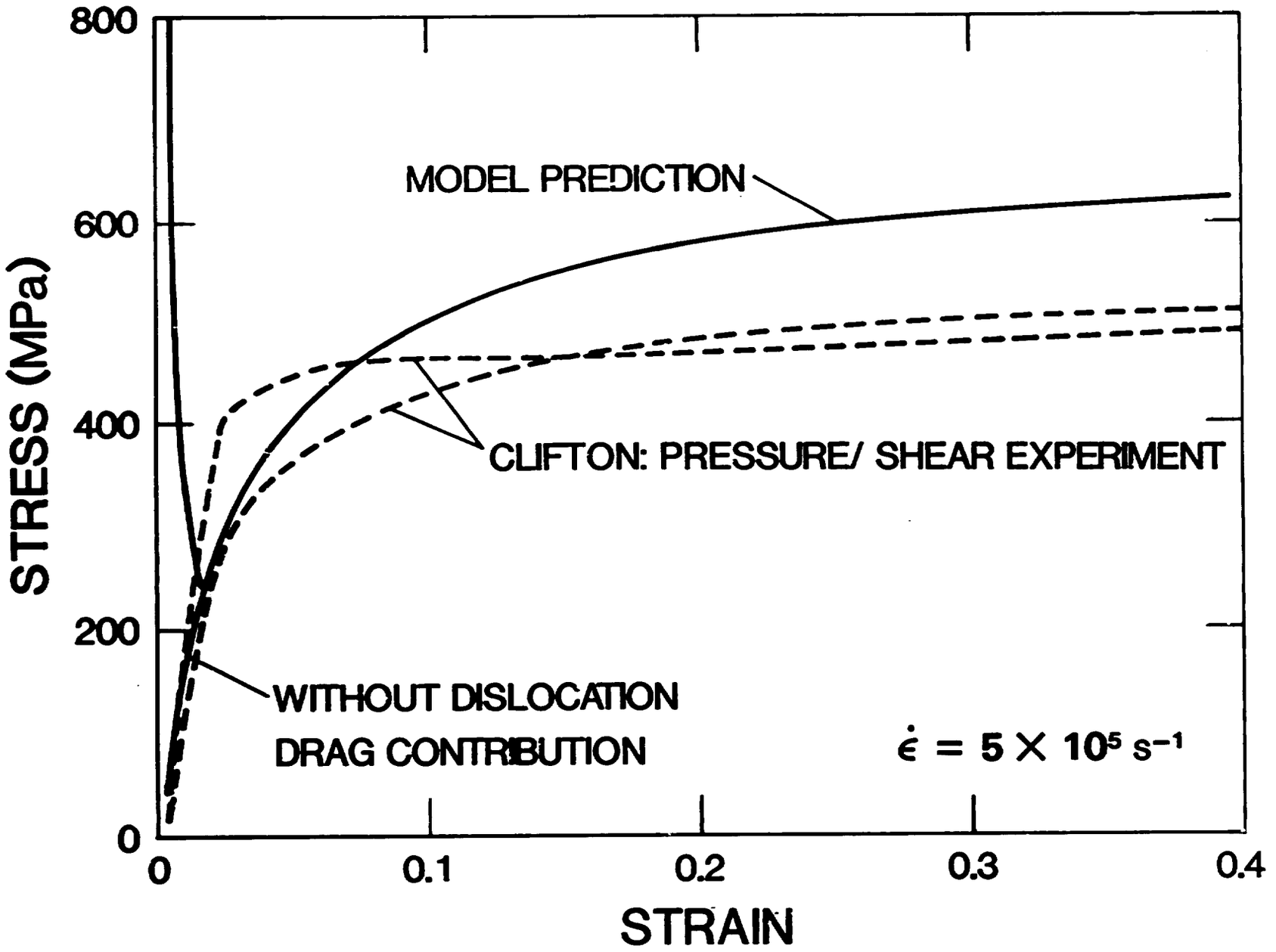
800
600
400
200
0
STRESS (MPa)
MODEL PREDICTION
CLIFTON: PRESSURE/ SHEAR EXPERIMENT
WITHOUT DISLOCATION
DRAG CONTRIBUTION
$\dot{\epsilon} = 5 \times 10^5\ s^{-1}$
0
0.1
0.2
0.3
0.4
STRAIN

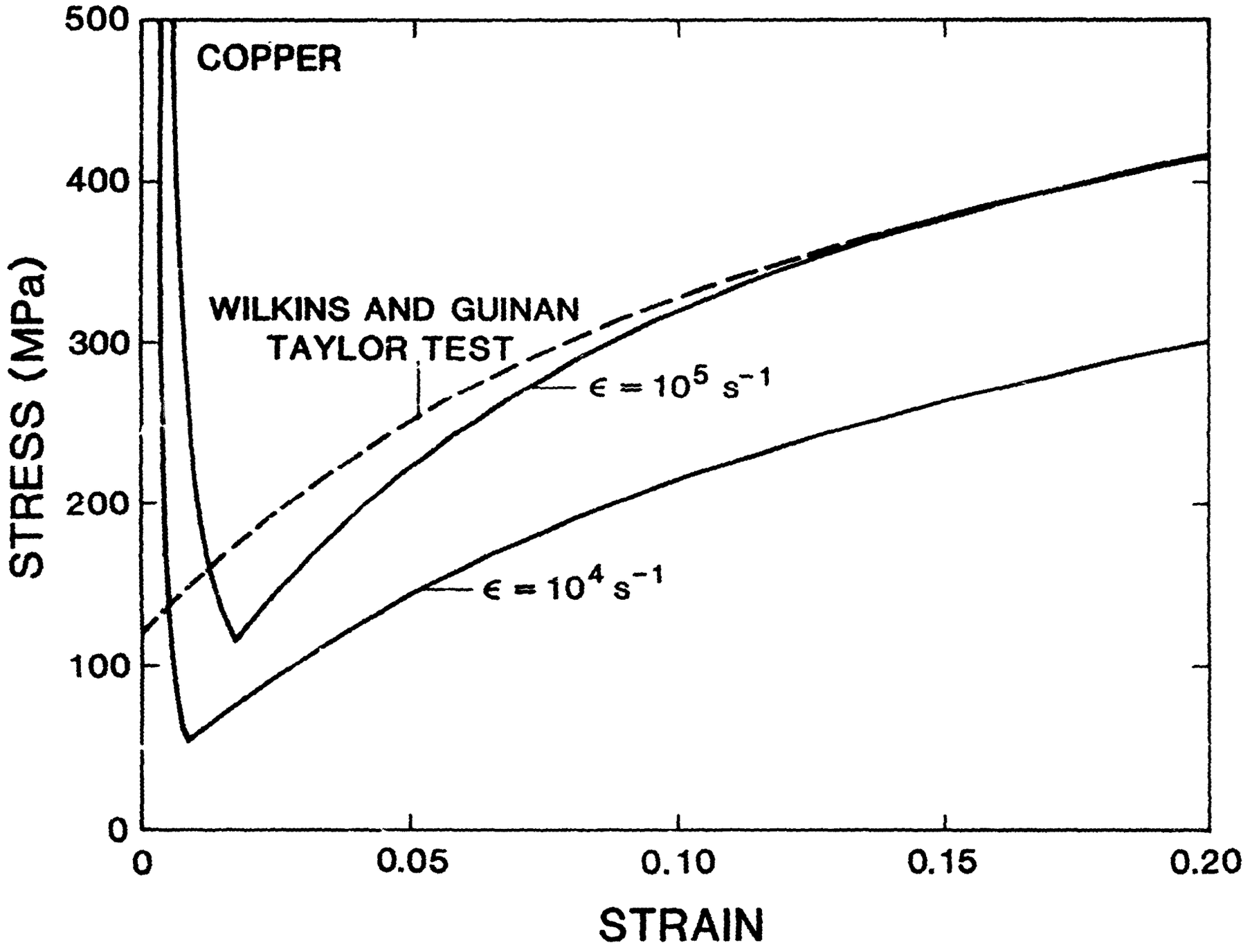
COPPER
WILKINS AND GUINAN
TAYLOR TEST
$\epsilon = 10^5\ s^{-1}$
$\epsilon = 10^4\ s^{-1}$
STRESS (MPa)
500
400
300
200
100
0
0
0.05
0.10
0.15
0.20
STRAIN

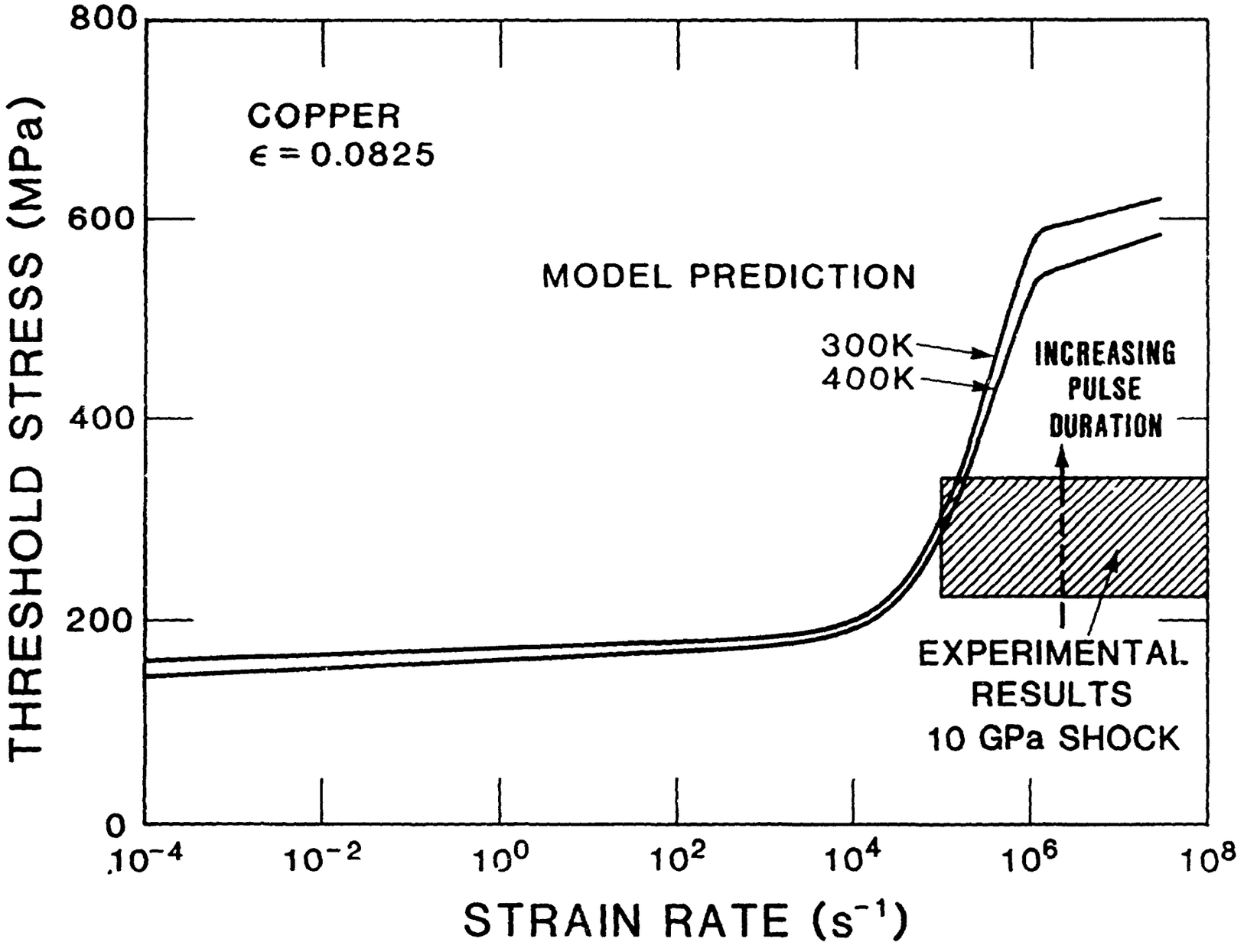
800
600
400
200
0
THRESHOLD STRESS (MPa)
COPPER
$\epsilon = 0.0825$
MODEL PREDICTION
300K
400K
INCREASING
PULSE
DURATION
EXPERIMENTAL
RESULTS
10 GPa SHOCK
10^{-4}
10^{-2}
10^{0}
10^{2}
10^{4}
10^{6}
10^{8}
STRAIN RATE (s^{-1})